Persistent draining crossover in DNA and other semi-flexible polymers: Evidence from hydrodynamic models and extensive measurements on DNA solutions

Marc L. Mansfield' , Achilleas Tsortos' , and Jack F. Douglas'

Citation: J. Chem. Phys. **143**, 124903 (2015); doi: 10.1063/1.4930918
View online: http://dx.doi.org/10.1063/1.4930918
View Table of Contents: http://aip.scitation.org/toc/jcp/143/12
Published by the American Institute of Physics

Persistent draining crossover in DNA and other semi-flexible polymers: Evidence from hydrodynamic models and extensive measurements on DNA solutions

Marc L. Mansfield,[1,a)] Achilleas Tsortos,[2,b)] and Jack F. Douglas[3,c)]
[1]*Bingham Research Center, Utah State University, Vernal, Utah 84078, USA*
[2]*Institute of Molecular Biology and Biotechnology, Foundation for Research and Technology—Hellas (FORTH), Vassilika Vouton, 70013 Heraklion, Greece*
[3]*Materials Science and Engineering Division, National Institutes of Standards and Technology, Gaithersburg, Maryland 20899, USA*

(Received 6 July 2015; accepted 18 August 2015; published online 24 September 2015)

Although the scaling theory of polymer solutions has had many successes, this type of argument is deficient when applied to hydrodynamic solution properties. Since the foundation of polymer science, it has been appreciated that measurements of polymer size from diffusivity, sedimentation, and solution viscosity reflect a convolution of effects relating to polymer geometry and the strength of the hydrodynamic interactions within the polymer coil, i.e., "draining." Specifically, when polymers are expanded either by self-excluded volume interactions or inherent chain stiffness, the hydrodynamic interactions within the coil become weaker. This means there is no general relationship between static and hydrodynamic size measurements, e.g., the radius of gyration and the hydrodynamic radius. We study this problem by examining the hydrodynamic properties of duplex DNA in solution over a wide range of molecular masses both by hydrodynamic modeling using a numerical path-integration method and by comparing with extensive experimental observations. We also considered how excluded volume interactions influence the solution properties of DNA and confirm that excluded volume interactions are rather weak in duplex DNA in solution so that the simple worm-like chain model without excluded volume gives a good leading-order description of DNA for molar masses up to 10^7 or 10^8 g/mol or contour lengths between 5 μm and 50 μm. Since draining must also depend on the detailed chain monomer structure, future work aiming to characterize polymers in solution through hydrodynamic measurements will have to more carefully consider the relation between chain molecular structure and hydrodynamic solution properties. In particular, scaling theory is inadequate for quantitative polymer characterization. [http://dx.doi.org/10.1063/1.4930918]

I. INTRODUCTION

Flexible polymers in solution having a sufficiently long chain length are expected to follow these asymptotic scaling laws,[1,2]

$$R_g \sim N^{\nu_R}, \tag{1}$$

$$R_h \sim N^{\nu_H}, \tag{2}$$

$$[\eta] \sim N^{3\nu_\eta - 1}, \tag{3}$$

$$S^0_{20,w} \sim N^{1-\nu_S}, \tag{4}$$

where R_g, R_h, [η], and $S^0_{20,w}$ represent the radius of gyration, the hydrodynamic radius, the intrinsic viscosity, and the sedimentation coefficient, respectively, where these properties are extrapolated to zero concentration ("infinite dilution") and where the sedimentation coefficient has been corrected to 20 °C in pure water. The static mass scaling exponent ν_R, defining the scaling of R_g with molecular mass in the limit of long polymer chains, equals $\nu_R = 0.5$ at the θ-point, where the effective excluded volume vanishes and is predicted to be $\nu_R \cong 0.59$ in good solvents where the chains are swollen relative to their ideal random coil dimensions.[1] Scaling arguments for the polymer size in solution normally assume that all exponents agree asymptotically: $\nu_R = \nu_H = \nu_\eta = \nu_S$. However, experiments often indicate discrepancies between the effective value of ν_R and the effective exponents ν_H, ν_η, or ν_S,[2] an effect historically interpreted in terms of hydrodynamic draining. (A discussion of the draining effect, its history, and various models of this phenomenon is given by Douglas and Freed.[3]) Regardless of interpretation, it is clear that these transport properties are slow to reach the "non-draining" or "fixed point" limit of the renormalization group theoretical description of polymer hydrodynamics[4] and we use the term "draining crossover" to refer to this effect.[5] While the word "crossover" implies that discrepancies with static scaling theory should disappear when the chain length N becomes large, the evidence indicates that this limit is often not obtainable for any reasonable molecular mass, i.e., the scaling limit cannot be experimentally realized.

We have developed a path-integration algorithm that calculates R_h and [η] for macromolecules of arbitrary shape,[5–10]

a)marc.mansfield@usu.edu
b)atsortos@imbb.forth.gr
c)jack.douglas@nist.gov

and it finds draining crossovers in the behavior of random coil polymers and other fractal objects.[5,11,12] The algorithm is exact within the electrostatic and Zimm rigid-body approximations which are, first, orientationally averaging the Oseen tensor and thereby converting it into the electrostatic Green's function,[13] and second, calculating transport properties of flexible macromolecules as ensemble averages over conformations with each conformation behaving as a rigid body. The success of the algorithm in treating many diverse macromolecular shapes validates the two approximations.[14]

The draining crossover is also apparent in experimental data on polymers. The θ- and good-solvent values of ν_R, 0.5 and ≅0.59, respectively, lead to the naïve expectation that intrinsic viscosity and hydrodynamic radius exponents, $3\nu_\eta - 1$ and ν_H, should be 0.5 each in θ-solvents, and ≅0.77 and ≅0.59 in good solvents.[2] However, effective exponents for flexible polymers in good solvents are usually smaller than the naïve scaling predictions,[2] while for stiff polymers, they are usually larger.[15] One of the largest R_h-R_g discrepancies occurs in DNA solutions, for which R_h exponents of about 0.6 and R_g exponents of about 0.52 have been reported over comparable chain lengths.[16–18] The impact of chain stiffness on the draining crossover is also clearly evidenced in our path-integration calculations.[5,11,12]

The draining crossover occurs because inter-segment effects (flow-field perturbations in the case of hydrodynamics and wave interference in the case of radiation scattering) on R_h and R_g are proportional to r^{-1} and r^2, respectively, where r is the distance between pairs of internal segments. This implies that transport properties are more sensitive to local contributions and that we must go to larger coils before asymptotic behavior is observed. With very stiff chains, the local segment density in the vicinity of any given segment is low, and inter-segment hydrodynamic effects are comparatively weak, while the converse is true for flexible chains. Our calculations imply the existence of a long-chain fixed point, with flexible chains and stiff chains approaching the fixed point from different directions: Flexible chains become more draining with increasing mass, while stiff chains become less draining. Hence, the effective exponents for stiff chains such as DNA are larger than the naïve expectation, while for flexible polymers, they are smaller.[5,15]

The draining crossover calls into question the decades old practice[19,20] of inferring metrical data for linear polymers from estimates of their transport properties that simply assumed the equality of static (radius of gyration and end-to-end distance) and dynamic measures of size from intrinsic viscosity, diffusion, and sedimentation measurements. Fortunately, this crossover effect normally has a secondary importance in flexible polymers so the failure of scaling theory is not so obvious.

The close proximity of the R_h exponent to the good-solvent value has led some to assert that DNA chains can be described as self-avoiding walks.[16,17] We have countered with the assertion that a draining crossover provides a better explanation of observations on DNA solution properties,[11] especially given abundant evidence that excluded volume interactions are weak in DNA.[18,21–24]

We have published two previous studies of stiff-chain analogs of duplex DNA in solution,[11,25] applying our path-integral formalism to the worm-like chain (WLC) model and to stiff or semi-flexible lattice chains where the chains in each case are taken to have a finite diameter. The lattice model was introduced to create longer chain configurations. In both these chain models, we neglected excluded volume interactions, since these interactions have been argued to be small in DNA[26] and because of the experimental evidence noted above.[18,21–24] In the present work, we revisit this question employing a large database of R_g, R_h, [η], and $S^0_{20,w}$ measurements that cover many orders of magnitude in chain length. We find excellent agreement between our ideal worm-like DNA models and this extensive data compilation and further confirm our previous conclusion that the discrepancy between the mass scaling of R_g and R_h in DNA solutions can be ascribed to a draining crossover. This comprehensive comparison between modeling and measurement confirms our former finding that excluded volume interactions are weak in DNA. As shown below, we find that excluded volume interactions are effectively absent in DNAs below a molar mass of 10^5 g/mol, are minimal in the range between 10^5 and 10^8 g/mol, and are probably not fully developed (i.e., displaying effective ν_R values near 0.59) until around 10^{10}–10^{11} g/mol.

λ-phage DNA has a molar mass of 3×10^7 g/mol, while samples generated there from by enzymatic digestion or ligase concatenation typically extend about one order of magnitude above or below this. Because they provide monodisperse chain length samples, these λ-phage DNA derivatives are popular sample systems for studying the physical properties of DNA.[16–18] Our finding is that they have at most a weak excluded volume interaction. (For comparison, the *E. coli* genome and human chromosome 1 have molar masses of 3×10^9 g/mol and 1.7×10^{11} g/mol, respectively.) We also consider a repulsive excluded volume interaction in the stiff lattice model and comment on the applicability of the worm-like chain to model DNA in solution when these excluded volume interactions are neglected.

II. MODEL DESCRIPTION

A. Worm-like chains

The WLC model treats polymers in solution as an ensemble of smoothly bending space curves in which the correlation in tangential direction is exponential,

$$\langle \mathbf{s}_1 \cdot \mathbf{s}_2 \rangle = e^{-|s_1 - s_2|/a}. \tag{5}$$

Here, a is the persistence length of the chain, and $\mathbf{s}_1$ and $\mathbf{s}_2$ denote the unit tangent vectors at any two points along the chain contour. The total contour length of the chain is L. The model comprehends rod-like polymers in one extreme, $L \ll a$, random coils in another, $L \gg a$, and all intermediate behavior between these two extremes. Whenever the chain thickness becomes relevant, we assume a circular cross section of diameter d. WLCs of finite diameter may be visualized as the volume swept out by a sphere of diameter d translating along any one of the space curves in the ensemble. The three parameters, a, L, and d, completely define the standard model. An excluded volume interaction would be imposed by removing from the ensemble any space curves that self-approach within

the distance d, but as is usually the case with excluded volume interactions, exact results are unavailable. Of course, excluded volume interactions are non-existent in the rod limit ($L \ll a$). None of the WLC results reported here include an excluded volume interaction. Elsewhere, we have reported calculations of R_h and [η] for the WLC model using our path-integration algorithm and worked out approximation schemes to represent the results.[25] For completeness, we reproduce those approximation schemes here. Our notation includes the following dimensionless ratios: $\varepsilon = a/L$ and $\delta = d/L$.

The well-known standard formula for R_g of the WLC is obtained by an appropriate integration of Eq. (5),

$$\frac{R^2_{g,thin}}{L^2} = \frac{2}{L^4}\int_0^L di \int_i^L dj \int_i^j dk \int_k^j dl e^{-(l-k)/a} = \frac{\varepsilon}{3} - \varepsilon^2 + 2\varepsilon^3 - 2\varepsilon^4\left(1 - e^{-1/\varepsilon}\right). \quad (6)$$

We denote this as $R^2_{g,thin}$ because it corresponds to the limit $d = 0$. However, as long as $L \gg d$, or $\delta \ll 1$, it is expected to be accurate. The following formula gives our correction[25] for larger δ:

$$R_g = R_{g,thin}\left(\frac{15 + 30\delta + 45\delta^2 + 18\delta^3}{15 + 10\delta}\right)^{1/2}. \quad (7)$$

We reemphasize that this formula neglects excluded volume.

The following equations represent our results[25] for R_h and [η] of ideal WLCs:

$$R_h = C_{rod}\left[\frac{1 + (0.038\,01)\, r_C^{-0.9212}}{1 + (0.072\,04)\, r_C^{-1.0204}}\right], \quad (8)$$

$$[\eta] = \frac{(0.79)\, N_A \alpha}{M}, \quad (9)$$

along with the auxiliary relations

$$r_C = \varepsilon\, \delta^{-0.134}, \quad (10)$$

$$C_{rod} = \frac{L}{2}(1+\delta)\left[t + \ln 4 - 1 - \frac{3.95}{t^2} + \frac{16.18}{t^3} - \frac{16}{t^4}\right]^{-1}, \quad (11)$$

$$\alpha = \alpha_{rod}\left[\frac{1 - (0.005\,690)\, r_\alpha^{-0.8350}}{1 + (0.2028)\, r_\alpha^{-1.0335}}\right], \quad (12)$$

$$r_\alpha = \epsilon \exp\left[(3.106)\, \delta^{1.213}\right], \quad (13)$$

$$\alpha_{rod} = L^3 \frac{\pi}{18}(1+\delta)^3 \times \left[t + \ln 4 - \frac{7}{3} - \frac{4.53}{t^{1.72}} + \frac{18.3}{t^{2.72}} - \frac{18}{t^{3.72}}\right]^{-1}, \quad (14)$$

$$t = \ln\left(1 + \frac{1}{\delta}\right). \quad (15)$$

M is the molar mass and N_A is the Avogadro's number. Eq. (9) is the intrinsic viscosity in practical (volume/mass) units: α has units of volume and N_A/M has units of mass^{-1}.

The sedimentation coefficient is determined by R_h,

$$S^0_{20,w} = \frac{BM}{6\pi N_A \eta_{20,w} R_h}. \quad (16)$$

Here, B is the buoyancy factor and $\eta_{20,w}$ is the viscosity of water at 20 °C (1.004 cp). The expressions for R_h, [η], and $S^0_{20,w}$ have only been tested for the parameter range,

$$10^{-4} < \delta < 0.1 \text{ and } \varepsilon > 0.025, \quad (17)$$

where we assume there is no excluded volume interaction. The R_g expression, Eq. (7), is expected to be valid over any chain length domain for which excluded volume is negligible and as long as Eq. (5) is valid.

Good fits to the empirical DNA data are obtained if we take $d = 2.4$ nm and $a = 50$ nm. The buoyancy factor B is taken to be 0.443, which is typical for DNA. The contour length is of course proportional to the number of base pairs and to the molar mass. We let n represent the number of base pairs, which we take to have units "bp." This formula gives the proportionalities between the three chain-length parameters,

$$n = \frac{M}{\left(663 \frac{\text{g}}{\text{mol·bp}}\right)} = \frac{L}{\left(0.340 \frac{\text{nm}}{\text{bp}}\right)}. \quad (18)$$

The restrictions, Eq. (17), on ε and δ translate into the following validity range for the application of Eqs. (8) and (9) to DNA: 80 bp $< n <$ 6000 bp, or 5×10^4 g/mol $< M < 4 \times 10^6$ g/mol.

B. Stiff (semi-flexible) lattice polymers

The criterion cited above, Eq. (17), restricting WLCs to ε > 0.025 (or $n <$ 6000 bp in the analogous DNA model) was dictated by the need during the path-integral calculation to represent each instance of a WLC as a collection of cylinders. To keep the worms as smoothly bending as possible required a large number of cylinders per persistence length. Worms with $L/a > 40$ required us to use so many cylinders that the calculation became prohibitively time-consuming.[25] To sample a higher range in L/a, we turned to stiff lattice chains (SLCs), i.e., stiff chains on a simple cubic lattice.[11] Each chain is modeled as a Markov walk on the lattice, but with a high probability for each step to be parallel to its predecessor, so that the resulting chains have persistence lengths equal to many lattice units. Immediate back-steps, in which a step is anti-parallel to its predecessor, are not allowed. In the path-integral calculation of the transport properties, each instance of a chain is represented as a collection of adjacent cubic lattice cells. Because the number of cubes per persistence length for the SLC is less than the number of cylinders per persistence length for the WLC, the SLC permits us to extend L/a by almost two orders of magnitude. Unless otherwise noted, the results appearing here are for chains without excluded volume.

The best match to the solution properties of DNA occurs when we adjust the bending energy such that the persistence length is 21 lattice units. We set the lattice unit to be 2.4 nm and assume 7.1 bp per lattice unit. If N is the number of lattice steps in the chain, then the contour length $L = (2.4\text{ nm})\, N$, and the persistence length is 21×2.4 nm = 50 nm. Semi-flexible lattice polymers with these characteristics give results for R_g, R_h, and [η] that correspond well to the continuum worm-like chain model.[11] We show results obtained earlier[11] for a DNA model equivalent to the SLC in Table I.

TABLE I. Results for the stiff lattice chain model,[11] in units appropriate for the equivalent DNA model.

n (bp)	M (g/mol)	R_g (nm)	R_h (nm)	[η] (dl/g)	$S^0_{20,w}$ (Sv)
142	9.4×10^4	12.7	7.5	0.47	4.8
370	2.4×10^5	29	14.4	1.61	6.6
710	4.7×10^5	48	23	3.5	8.1
1 420	9.4×10^5	78	37	7.4	9.9
3 600	2.4×10^6	132	68	16.6	13.5
7 100	4.7×10^6	200	107	30	17.1
14 200	9.4×10^6	280	164	51	22
36 000	2.4×10^7	450	280	96	32
71 000	4.7×10^7	640	420	148	44
142 000	9.4×10^7	900	620	230	59
360 000	2.4×10^8	1430	1020	390	90

C. Smooth versus abrupt chain bending

Both the WLC and the SLC are rod-like at low chain lengths and random coils in the long chain limit, but one becomes flexible by bending smoothly, the other by bending abruptly. Good agreement between models with smooth and abrupt bending has been discussed previously by one of us.[27] We see that R_g values estimated from these two models are in excellent agreement because tangential correlations along the chain in both cases are exponential, as in Eq. (5). For the lattice model, the integrals in Eq. (6) are replaced by discrete sums, but in the stiff limit and in the limit of large n, the sums and integrals agree very well. The reason for agreement between the transport properties is not so transparent. It probably results because $\langle r^{-1} \rangle$ moments in both models agree reasonably well. We are not asserting that the two models are entirely interchangeable, but that both represent global properties of DNA.[27]

Of course, we can only claim good agreement between the WLC and the SLC over the chain length range for which both were studied. However, it seems reasonable to assume that the greatest discrepancies between the two models occur at lower chain lengths, and that the WLC and the SLC are in good general agreement, for global properties such as R_g, R_h, or [η], at all lengths.

III. EXCLUDED VOLUME INTERACTIONS IN THE STIFF (SEMI-FLEXIBLE) LATTICE POLYMER MODEL

As previously mentioned, most of the applications of the two models considered here are without excluded volume interactions. To determine whether such neglect is appropriate, we have calculated the radius-of-gyration expansion factor for the stiff lattice chain,

$$\alpha_R = \frac{R_{g,ex}}{R_{g,0}}, \tag{19}$$

where $R_{g,0}$ and $R_{g,ex}$ represent, respectively, the radius of gyration taken over the full ensemble of Markov walks and that taken over the ensemble that excludes self-intersecting chains. The results of this analysis are shown in Figure 1. When N is below about 4000, excellent statistics are obtained by generating an ensemble of chains as Markov walks on the lattice, and then extracting the sub-ensemble of chains without self-intersections. That this works is, in itself, evidence that excluded volume interactions are weak. Above $N = 4000$, chains were generated by the pivot algorithm.[28] The fundamental pivot move consists of all possible rotations and mirror-inversions on the lattice. We were able to simulate chain lengths as large as $N = 2.9 \times 10^5$, corresponding to a DNA-equivalent molar mass of 1.37×10^9 g/mol. Higher chain lengths were attempted, but the calculations never converged. Below a molar mass of 10^5 g/mol, the expansion factor α_R is near 1, while over the molar mass range 2×10^5 g/mol–3×10^7 g/mol, α_R depends on M with an effective exponent of only 0.01. In the vicinity of 10^9 g/mol, or the upper extent of our calculations, the effective exponent is about 0.045, still weaker than the expected asymptotic behavior $\alpha_R \sim M^{0.088}$.

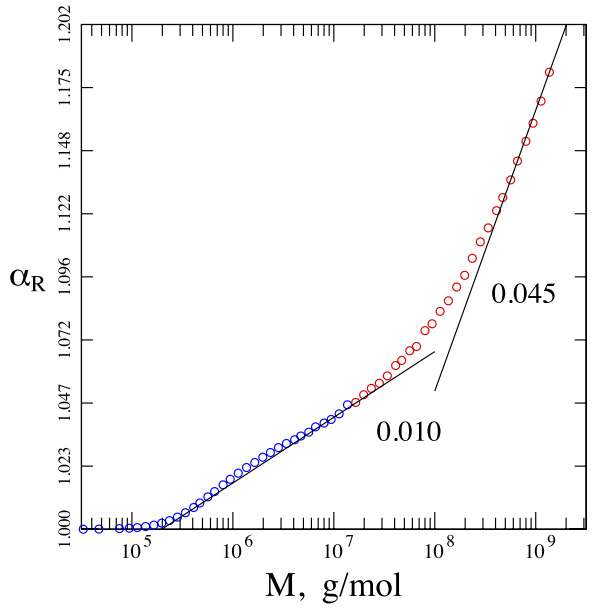

FIG. 1. Radius-of-gyration expansion factor for the stiff lattice chain model as a function of the DNA-equivalent molar mass. Both the ordinate and the abscissa are logarithmic. Blue symbols were calculated by generating an ensemble of Markov chains on the lattice and then discarding those with self-intersections. Red symbols were calculated by the pivot algorithm. Two approximate tangent lines have the indicated slopes.

Figure 2 provides another representation of the expansion-factor results. It displays $\partial \log_{10} R_g / \partial \log_{10} M$ as a function of M. Therefore, it gives the instantaneous slope of a log-log plot of R_g vs. M. The solid blue curve was calculated using Eq. (6) and therefore represents the behavior expected in the absence of excluded volume. It shows the rod-coil transition as the slope changes from near 1 at low M to 0.5 at high M. The red symbols were calculated from the expansion-factor results of Figure 1 and therefore give the effective R_g-M exponent in the presence of excluded volume. Evidently, excluded volume effects become appreciable only for extremely large M, i.e., $M > 10^7$ g/mol. The scaling-law expectation of 0.588 appears as a horizontal dashed line. The red symbols behave as if they will level off at the expected asymptote of $\nu = 0.588$, but perhaps not before $M = 10^{10}$ or 10^{11} g/mol. The most extensive molar mass range examined experimentally[16–18] is that typical of λ-phage DNA and its enzymatic digests or concatenates, i.e., 10^6–10^8 g/mol, over which the effective exponent for α_R is only 0.01.

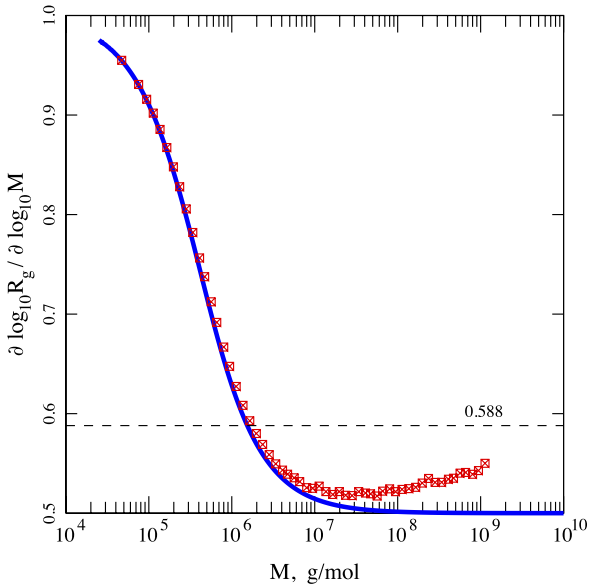

FIG. 2. Plot of $\partial \log_{10} R_g / \partial \log_{10} M$ — the instantaneous slope of the log-log plot of R_g vs. M — for the worm-like chain model (blue curve) and the stiff lattice chain model with excluded volume (red symbols). M is the molar mass of the equivalent DNA chain. The dashed line is the anticipated exponent for self-avoiding flexible polymers, $\nu = 0.588$.

IV. DRAINING CROSSOVER EFFECT

Figures 3 and 4 display the dimensionless ratios R_h/R_g and $m\,[\eta]/R_g^3$ (m denotes polymer molecular mass) for the WLC and SLC models plotted against the DNA-equivalent molar mass. The minima in the two curves occur because of the transition from rod-to-coil behavior. WLCs in the short-rod extreme ($L \approx d \ll a$) or in the random coil extreme ($d \ll a \approx L$) are less anisotropic than when ($d \ll a \approx L$). Because shape anisotropy influences these dimensionless ratios,[12] the minima are expected for L on the order $L \sim \mathrm{O}(a)$, and indeed, the minima occur when $L \approx 5a$.

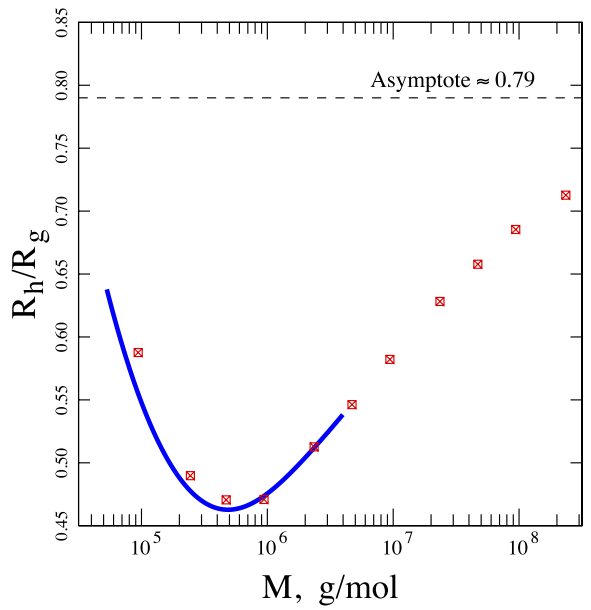

FIG. 3. Dimensionless ratio R_h/R_g for the worm-like chain model (blue curve) and stiff lattice chain model (red symbols) vs. DNA-equivalent molar mass, M. The $M \to \infty$ asymptote is also shown.

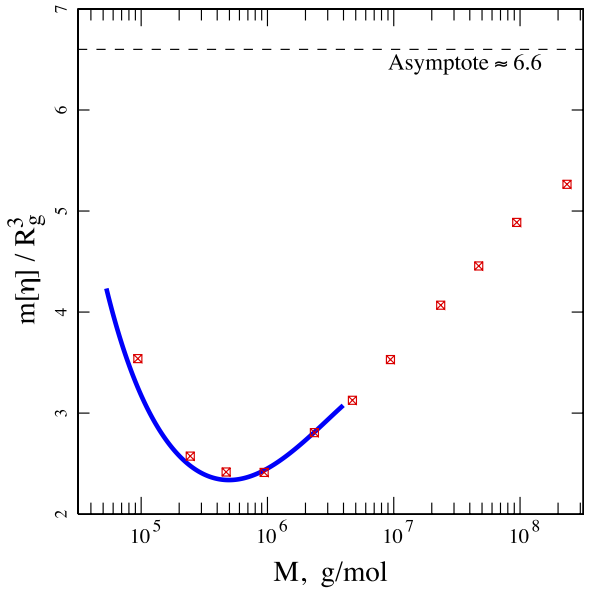

FIG. 4. Dimensionless ratio $m[\eta]/R_g^3$ for the worm-like chain model (blue curve) and stiff lattice chain model (red symbols) vs. DNA-equivalent molar mass, M. m is the molecule mass, and the asymptote for $M \to \infty$ is indicated.

In the limit of large M, these ratios asymptotically approach constant values, $R_h/R_g \approx 0.79$ and $m\,[\eta]/R_g^3 \approx 6.6$.[5] Figures 3 and 4 suggest that the WLC eventually reaches its asymptotic scaling limit, but this obviously has not occurred for $M = 2.5 \times 10^8$ g/mol or equivalently 4×10^5 base pairs.

V. COMPARISON WITH EXPERIMENT

We have gathered aqueous DNA solution data from many sources for R_g,[18,29–34] for R_h,[16,17,35–46] for [η],[47] and for $S^0_{20,w}$ [29,30,48–50] and compared these results with the models presented above in Figure 5. In all cases, the data correspond to physiological salt concentration. Each of these studies should be consulted regarding the estimations on measurement uncertainty. Here, we display $S^0_{20,w}$ data along with R_h data since this conversion between these properties involves model assumptions. Figure 5 displays good agreement between experimental data and the predictions of the SLC model over orders of magnitude in chain length. Because of modeling restrictions mentioned above, comparisons against WLC model predictions are confined to about two orders of magnitude in chain length. Two R_g data points at low M agree better with the $R_{g,thin}$ result than with the finite-thickness correction, a finding that we attribute to probable experimental errors in these observations.

As pointed out before by Tsortos *et al.*,[47] and illustrated in Figure 5, a break occurs in the [η] trace at about $M = 2 \times 10^6$ g/mol or about $n = 3000$ base-pairs, with effective Mark-Houwink exponents below and above taking values of 0.69 and 1.05, respectively. The break occurs within the domain for which α_R of the equivalent lattice model scales as $M^{0.01}$ (see Figure 1), meaning that the excluded volume interaction is extremely weak in this regime. Therefore, the break-point should not be interpreted as a crossover associated with excluded-volume but rather reflects a transition in conformational structure from a more rod-like form to a worm-like coil. In any case, the curvature in the Mark-Houwink curve is not

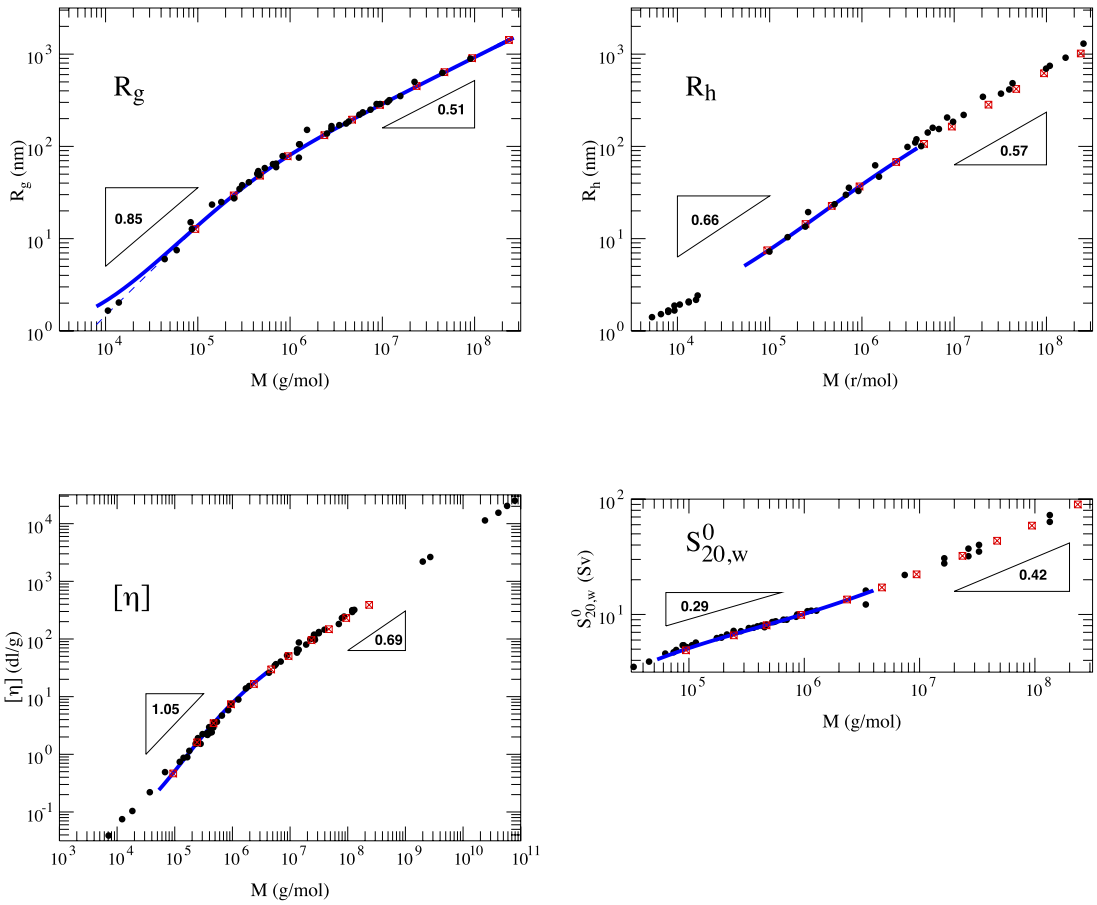

FIG. 5. Comparison between experimental data (black circles) and the predictions of the worm-like chain model (blue traces) and the stiff lattice chain model (red symbols) for R_g, R_h, [η], and $S^0_{20,w}$. The dashed blue curve in the R_g panel at low M is the $R_{g,thin}$ prediction, Eq. (6), while the solid curve is R_g as calculated by Eq. (7). Effective slopes of the experimental data above and below a molar mass of 2×10^6 g/mol are also shown.

surprising given the strong departure of the chain conformational structure from an ideal random coil or self-avoiding walk.

VI. SUMMARY AND CONCLUSIONS

There is good agreement between the WLC and SLC models at all chain lengths studied, out to a molar mass of 4×10^6 g/mol, for the properties R_g, R_h, and [η]. As mentioned above, it is reasonable to assume that the two models agree at all higher molar masses. The primary difference between the two models is that one bends smoothly while the other bends abruptly. This indicates that measurements such as R_g, R_h, and [η] are unable to distinguish between these modes of bending (see also Ref. 27).

The WLC successfully predicts R_h and [η] of DNA in solution at molar masses between 5×10^4 g/mol and 4×10^6 g/mol, and it predicts R_g at molar masses between 8×10^3 g/mol and 2×10^8 g/mol. The SLC successfully predicts R_h and [η] of DNA between 1×10^5 g/mol and 2×10^8 g/mol.

DNA molecules in aqueous solutions with moderate salt concentrations apparently exhibit three regimes associated with changes in configurational structure with increasing molar mass: a rod-to-worm-like chain transition regime, a semi-flexible chain to random coil regime, and a theoretical self-avoiding chain regime for astronomical chain lengths. The end of the first regime can be specified by the minimum in R_h/R_g in Fig. 3 near for M $\approx 1 \times 10^5$ g/mol, and the cross-over to a random coil may be estimated by the point in Figure 2 at which the ν_R approaches 0.5, corresponding to $M \approx 1 \times 10^7$ g/mol. Figures 3 and 4 imply that the draining crossover only becomes complete for $M \gg 2 \times 10^8$ g/mol, while Figure 2 implies that a crossover to the asymptotic good-solvent scaling limit must involve chains longer than $M = 10^9$ g/mol. This last regime is not accessible in our simulations and in the range of DNA masses investigated experimentally. Moreover, the hydrodynamic interaction strength is weak in *all* these extended polymer structures, and this effect is complicated by the fact that the hydrodynamic interaction strength should be *variable* in each regime because of the change of conformational structure with M. It then is no surprise that naïve scaling relation between hydrodynamic properties and R_g do not apply to DNA.

We also observe from Figure 2 that excluded-volume effects are not detectable below $M \approx 3 \times 10^7$ g/mol so that the worm-like chain model without excluded volume is an appropriate model below this rather large DNA mass. Figure 5 indicates that this model continues to accord with observations even for M as large as 2×10^8 g/mol. We suggest that a fully developed excluded volume regime, as evidenced by a scaling $R_g \sim N^{0.59}$, should correspond to M larger 10^{10} or 10^{11} g/mol. We then conclude that excluded volume interactions in DNA

can be safely ignored to a first order approximation and that DNA molecules should not be considered to be self-avoiding walks in bulk solutions under the salt conditions normally investigated. This conclusion should not be extended to DNA under high confinement (scales on the order of the persistence length a) since the strength of the excluded volume interaction should be greatly amplified under these conditions.[51] Our conclusions also do not apply to low salt conditions where long-range electrostatic interactions must have an appreciable effect on the dimensions of DNA.

ACKNOWLEDGMENTS

M.L.M. acknowledges financial support from the Utah Science Technology and Research (USTAR) initiative. A.T. acknowledges financial support from the European Union FP7 grant: REGPOT-"InnovCrete" (Contract No. 316223).

[1]K. F. Freed, *Renormalization Group Theory of Macromolecules* (John Wiley & Sons, New York, 1987).
[2]P.-G. de Gennes, *Scaling Concepts in Polymer Physics* (Cornell University Press, Ithaca, New York, 1979), p. 38.
[3]J. F. Douglas and K. F. Freed, Macromolecules **27**, 6088–6099 (1994).
[4]S.-Q. Wang, J. F. Douglas, and K. F. Freed, J. Chem. Phys. **87**, 1346 (1984).
[5]M. L. Mansfield and J. F. Douglas, Phys. Rev. E **81**, 021803 (2010).
[6]M. L. Mansfield, J. F. Douglas, and E. J. Garboczi, Phys. Rev. E **64**, 061401 (2001).
[7]M. L. Mansfield and J. F. Douglas, Condens. Matter Phys. **5**, 249 (2002).
[8]E.-H. Kang, M. L. Mansfield, and J. F. Douglas, Phys. Rev. E **69**, 031918 (2004).
[9]M. L. Mansfield, J. F. Douglas, S. Irfan, and E.-H. Kang, Macromolecules **40**, 2575–2589 (2007).
[10]M. L. Mansfield and J. F. Douglas, Phys. Rev. E **78**, 046712 (2008).
[11]M. L. Mansfield and J. F. Douglas, Soft Matter **9**, 8914–8922 (2013).
[12]M. L. Mansfield and J. F. Douglas, J. Chem. Phys. **139**, 044901 (2013).
[13]J. B. Hubbard and J. F. Douglas, Phys. Rev. E **47**, R2983–R2986 (1993).
[14]B. H. Zimm, Macromolecules **13**, 592–602 (1980).
[15]A. Dondos and G. Staikos, Colloid Polym. Sci. **273**, 626–632 (1995).
[16]D. E. Smith, T. T. Perkins, and S. Chu, Macromolecules **29**, 1372–1373 (1996).
[17]R. M. Robertson, S. Laib, and D. E. Smith, Proc. Natl. Acad. Sci. U. S. A. **103**, 7310–7314 (2006).
[18]M. Nepal, A. Yaniv, E. Shafran, and O. Krichevsky, Phys. Rev. Lett. **110**, 058102 (2013).
[19]P. J. Flory, in *Statistical Mechanics of Chain Molecules* (Wiley, New York, 1969), Chap. II.
[20]H. Morawetz, in *Macromolecules in Solution*, 2nd ed. (Wiley, New York, 1975), Chap. VI.
[21]X. Qiu, K. Andresen, L. W. Kwok, J. S. Lamb, H. Y. Park, and L. Pollack, Phys. Rev. Lett. **99**, 038104 (2007).
[22]E. Shafran, A. Yaniv, and O. Krichevsky, Phys. Rev. Lett. **104**, 128101 (2010).
[23]D. Bracha, E. Karzbrun, G. Shemer, P. A. Pincus, and R. H. Bar-Ziv, Proc. Natl. Acad. Sci. U. S. A. **110**, 4534–4538 (2013).
[24]D. R. Tree, A. Muralidhar, P. S. Doyle, and K. D. Dorfman, Macromolecules **46**, 8369–8382 (2013).
[25]M. L. Mansfield and J. F. Douglas, Macromolecules **41**, 5412–5421 (2008).
[26]H. Yamakawa and W. H. Stockmayer, J. Chem. Phys. **57**, 2843 (1972).
[27]M. L. Mansfield, Macromolecules **19**, 854–859 (1986).
[28]*Monte Carlo and Molecular Dynamics Simulations in Polymer Science*, edited by K. Binder (Oxford University Press, Oxford, 1995).
[29]P. Doty, B. B. McGill, and S. A. Rice, Proc. Natl. Acad. Sci. U. S. A. **44**, 432–438 (1958).
[30]J. E. Godfrey and H. Eisenberg, Biophys. Chem. **5**, 301–318 (1976).
[31]H. Lederer, R. P. May, J. K. Kjems, G. Baer, and H. Heumann, Eur. J. Biochem. **161**, 191–196 (1986).
[32]K. Fukudome, K. Yamaoka, and H. Ochiai, Polym. J. **19**, 1385–1394 (1987).
[33]C. Yuan, H. Chen, X. W. Lou, and L. A. Archer, Phys. Rev. Lett. **100**, 018102 (2008).
[34]N. Rawat and P. Biswas, J. Chem. Phys. **131**, 165104 (2009).
[35]G. Voordouw, Z. Kam, N. Borochov, and H. Eisenberg, Biophys. Chem. **8**, 171–189 (1978).
[36]K. Soda and A. Wada, Biophys. Chem. **20**, 185–200 (1984).
[37]S. S. Sorlie and R. Pecora, Macromolecules **23**, 487–497 (1990).
[38]W. Eimer and R. Pecora, J. Chem. Phys. **94**, 2324–2329 (1991).
[39]H. T. Goinga and R. Pecora, Macromolecules **24**, 6128–6138 (1991).
[40]J. Seils and T. Dorfmüller, Biopolymers **31**, 813–825 (1991).
[41]T. Nicolai and M. Mandel, Macromolecules **22**, 2348–2356 (1989).
[42]U.-S. Kim, B. S. Fujimoto, C. E. Furlong, J. A. Sundstrom, R. Humbert, D. C. Teller, and J. M. Schurr, Biopolymers **33**, 1725–1745 (1993).
[43]G. F. Bonifacio, T. Brown, G. L. Conn, and A. N. Lane, Biophys. J. **73**, 1532–1583 (1997).
[44]J. Lapham, J. P. Rife, P. B. Moore, and D. M. Crothers, J. Biomol. NMR **10**, 255–262 (1997).
[45]V. M. Marathias, B. Jerkovic, H. Arthanari, and P. H. Bolton, Biochemistry **39**, 153–160 (2000).
[46]A. E. Nkodo, J. M. Garnier, B. Tinland, H. Ren, C. Desruisseaux, L. C. McCormick, G. Drouin, and G. W. Slater, Electrophoresis **22**, 2424–2432 (2001).
[47]A. Tsortos, G. Papadakis, and E. Gizeli, Biopolymers **95**, 824–832 (2011), and references cited therein.
[48]F. W. Studier, J. Mol. Biol. **11**, 373–390 (1965).
[49]M. T. Record, Jr., C. P. Woodbury, and R. B. Inman, Biopolymers **14**, 393–408 (1975).
[50]R. T. Kovacic and K. E. Van Holde, Biochemistry **16**, 1490–1498 (1977).
[51]F. Vargas-Lara, S. M. Stavis, E. A. Strychalski, B. J. Nablo, J. Geist, F. W. Starr, and J. F. Douglas, "Dimensional reduction of duplex DNA under confinement to nanofluidic slits," Soft Matter (to be published).